Available online at www.sciencedirect.com
SCIENCE DIRECT
Biomaterials 27 (2006) 5277–5285
Biomaterials
www.elsevier.com/locate/biomaterials

Synthesis of cell-adhesive dextran hydrogels and macroporous scaffolds

Stéphane G. Lévesque[a,c], Molly S. Shoichet[a,b,c,*]

[a]Department of Chemical Engineering and Applied Chemistry, University of Toronto, 200 College Street, Toronto, Ont., Canada M5S 3E5
[b]Department of Chemistry, University of Toronto, 80 St. George St., Toronto, Ont., Canada M5S 3H6
[c]Institute of Biomaterials and Biomedical Engineering, University of Toronto, 4 Taddle Creek Road, Toronto, Ont., Canada M5S 3G9

Received 13 February 2006; accepted 5 June 2006
Available online 21 June 2006

Abstract

Dextran hydrogels have been previously investigated as drug delivery vehicles and more recently as macroporous scaffolds; however, the non-cell-adhesive nature of dextran has limited its utility for tissue engineering. To overcome this limitation, macroporous scaffolds of methacrylated dextran (Dex-MA) copolymerized with aminoethyl methacrylate (AEMA) were synthesized, thereby introducing primary amine groups for covalent immobilization of extracellular-matrix-derived peptides. The amino group density for hydrogels copolymerized with 0.5 wt% AEMA was found to be $36.1 \pm 0.4\,\mu mol/cm^3$ by elemental analysis. To further enhance cellular interaction, poly(Dex-MA-*co*-AEMA) hydrogels were modified with either C**RGD**S or a mixture of CDPG**YIGSR** and CQAAS**IKVAV** (1:1, v/v) using sulfo-(*N*-maleimidomethyl)cyclohexane-1-carboxylate (sulfo-SMCC). The immobilized peptide concentration was determined using amino acid analysis at: $2.6 \pm 0.9\,\mu mol/cm^3$ for C**RGD**S-derived hydrogels and $2.2 \pm 0.3\,\mu mol/cm^3$ plus $1.9 \pm 0.2\,\mu mol/cm^3$ for CDPG**YIGSR** plus CQAAS**IKVAV**-derived hydrogels, respectively. Cellular interactions of primary embryonic chick dorsal root ganglia (DRGs) were compared on the hydrogels. Cell adhesion and neurite outgrowth on poly(Dex-MA) increased with copolymerization of AEMA and further improved with peptide modification and significantly for CDPG**YIGSR**/CQAAS**IKVAV**-derived poly(Dex-MA-*co*-AEMA) hydrogels. Moreover, DRGs penetrated within the first 600 μm of the scaffolds, thereby demonstrating the potential of this scaffold for guided cell and axonal regeneration in vivo.

Keywords: Dextran; Cell adhesion; Macroporous structure; Nerve tissue engineering

1. Introduction

Dextran, which consists of α-1,6-linked D-glucopyranose residues, is a bacterial-derived polysaccharide generally produced by enzymes from certain strains of *Leuconostoc* or *Streptococcus*. Crosslinked dextran hydrogel beads have been widely used as low protein-binding matrices for column chromatography applications (Sephadex®) [1–4] and for microcarrier cell culture technology (Cytodex™) [5–7]. More recently, dextran hydrogels have been considered for biomaterials applications [8–20] and investigated as drug delivery vehicles [21–31]. They are particularly compelling as scaffolds for soft tissue-engineering applications because dextran is resistant to both protein adsorption [32] and cell-adhesion [11,33,34], allowing cell adhesion to be achieved by specific derivatization with extracellular matrix (ECM)-based peptides [34,35].

We previously reported a method to create macroporous, interconnected dextran scaffolds by taking advantage of the polymer–polymer immiscibility of aqueous solutions of PEG and Dex-MA during polymerization across the methacrylate groups [36]. While these scaffolds had an interesting morphology, their use in tissue engineering was limited by poor cell adhesion. To overcome this limitation, the copolymerization of Dex-MA with AEMA was investigated by first creating a macroporous scaffold and then introducing primary amine groups to provide reactive anchors for covalent attachment of ECM-derived peptides.

The use of ECM proteins and peptides has been well established in tissue-engineering strategies [37–40] and

*Corresponding author. Terrence Donnelly Centre for Cellular and Biomolecular Research, University of Toronto, 160 College Street, Room 514, Toronto, Ont., Canada M5S 3E1. Tel.: +1 416 978 1460; fax: +1 416 978 4317.
E-mail address: molly@ecf.utoronto.ca (M.S. Shoichet).

0142-9612/$ - see front matter © 2006 Elsevier Ltd. All rights reserved.
doi:10.1016/j.biomaterials.2006.06.004

numerous studies have focused on facilitating neurite growth on ECM-modified biomaterials[41–49]. The most commonly studied ECM-derived proteins and peptides include fibronectin [50], the fibronectin-derived RGD peptide sequence [35,43,48,50–57], laminin [44], the laminin-derived YIGSR peptide sequence [43–47,49,53,56,57], and the laminin-derived IKVAV peptide sequence [35,43,44,46,47,49,56,57].

Previously we demonstrated that while G**YIGSR**-modified surfaces led to greater cell adhesion and S**IKVAV**-modified surfaces promoted greater neurite outgrowth [58], surfaces modified with both G**YIGSR** and S**IKVAV** had a synergistic effect on neurite outgrowth [47]. Moreover, surfaces modified with extended laminin-derived oligopeptides, CDPG**YIGSR** and CQAAS**IKVAV**, which better mimic the native region conformation of the active sites, promoted a greater cellular response than those modified with the respective minimal peptide sequences [46].

Polysaccharide hydrogels have been previously functionalized by covalently attaching cell-adhesive peptides to hydroxyl, amino, or carboxyl groups via zero-length crosslinking agents such as carbodiimides [44,45,52,55]. In addition, G**RGDS**P [34,35] and SRARKQAAS**IKVAV**-SADR [35] have been coupled to dextran by reacting primary peptide amines with hemiacetals of oxidized dextran. However, none of these approaches preserve the conformation of the peptides when amine-pendant groups are present (such as in the side-chain of lysine), which limits cell receptor interactions.

To overcome the limitations of these methods, sulfo-succinimidyl-4-(*N*-maleimidomethyl)cyclohexane-1-carboxylate (sulfo-SMCC) [46,49] was used to crosslink primary amines of poly(Dex-MA-*co*-AEMA) with sulfhydryl-terminated peptides, i.e., CG**RGDS**, CGDPG**YIGSR** and CQAAS**IKVAV**. Cell adhesion and neurite outgrowth of DRGs were compared quantitatively in vitro on peptide-modified hydrogels and for cell/neurite penetration on similarly modified scaffolds.

2. Materials and methods

2.1. Materials

All chemicals were purchased from Sigma-Aldrich Canada Ltd. (Oakville, Ont.) and used as received, unless otherwise noted. Water was distilled and deionized using a Millipore Milli-RO 10 Plus system at 18 MΩ resistance. Aqueous solutions of ammonium persulfate (APS) and tetramethylethylene diamine (TEMED) were prepared immediately prior to each use.

2.2. Synthesis of methacrylated dextran (Dex-MA)

Dex-MA was synthesized by modifying dextran with glycidyl methacrylate (GMA) as previously described to a degree of substitution (DS) of 10 [36]. Briefly, 5 g of dextran 6 kDa (*Leuconostoc mesenteroides*) was dissolved under nitrogen in 50 ml of anhydrous dimethylsulfoxide (DMSO) followed by the addition of 1 g of 4-dimethylaminopyridine (DMAP). GMA (688 μl) was then added to the solution. The mixture was stirred at room temperature for 48 h after which DMAP was neutralized by adding an equimolar amount of concentrated HCl. The dextran solution was dialyzed against distilled water at 4 °C, lyophilized and stored at −20 °C. The DS was confirmed by proton nuclear magnetic resonance (^{1}H-NMR) as previously described [36] using a Gemini 300 MHz spectrometer (Varian Associates, Inc. NMR Instruments, Palo Alto, CA) with D_2O as the solvent [59].

2.3. Synthesis of cell-adhesive peptides

Three ECM-derived peptides, H_2N–C**RGDS**–COOH, H_2N–CDPG**YIGSR**–COOH and, H_2N–CQAAS**IKVAV**–COOH, were custom-synthesized by solid-phase synthesis with standard FMOC/HATU chemistry (Pioneer™ Peptide Synthesis System, Applied Biosystems, Foster City, CA). Amino acids were purchased from Novabiochem (EMD Biosciences, Inc., La Jolla, CA). Activators and resins were purchased from Applied Biosystems and *N,N*-dimethylformamide (DMF) was purchased from Caledon Laboratories Ltd. (Georgetown, Ont.).

The peptides were cleaved and deprotected from the resin for 2 h using a cleavage cocktail of 88% trifluoroacetic acid (TFA; Caledon Laboratories Ltd.), 5% H_2O, 5% phenol, and 2% triisopropylsilane. Peptides were precipitated in cold diethyl ether, dried, re-dissolved in water, and then purified by reverse phase high-performance liquid chromatography (RP-HPLC, VP Series HPLC workstation, Shimadzu Scientific Instruments, Inc., Columbia, MD) using a Phenomenex® Jupiter™ preparative C18 column (5 μm, 300 Å, 250 × 21.2 mm, Phenomenex®, Torrance, CA). Molecular weights of the peptides were confirmed by mass spectrometry.

2.4. Preparation of poly(Dex-MA-co-AEMA) scaffolds and hydrogels

Dex-MA was copolymerized with aminoethyl methacrylate (AEMA) (Pierce Chemical Co., Rockford, IL) in a cylindrical glass mold in the presence of excess water and poly(ethylene glycol) (PEG, 10 kDa) by adapting a previously described methodology [36]. Briefly, solutions of 10 wt% Dex-MA and 5 wt% PEG were prepared with different concentrations of AEMA (0.1, 0.25 and 0.5 wt%). The solutions were mixed by vortex for 2 min followed by the addition of 10 wt% APS and 1.4 wt% TEMED (where the wt% of the initiator is relative to the mass of GMA coupled to Dex-MA). The solutions were briefly mixed by vortex again and injected into the glass mold, which was barreled at 40 rpm overnight. All scaffolds were washed with deionized water and were allowed to swell in water for 1 week, with daily water exchanges. The synthesis was repeated in the absence of PEG which led to the formation of hydrogels (and not scaffolds). From hereon, scaffolds will refer to macroporous structures formed in the presence of PEG while hydrogels will refer to those structures formed in the absence of PEG.

2.5. Characterization of poly(Dex-MA-co-AEMA) scaffolds

The morphology of poly(Dex-MA-*co*-AEMA) scaffolds was characterized by scanning electron microscopy (SEM) while swellability was determined by equilibrium water content (EWC). For morphological analysis, cross-sections of poly(Dex-MA-*co*-AEMA) scaffolds were mounted onto aluminum studs and sputter-coated with gold for 180 s. The scaffold morphology was examined under a scanning electron microscope (SEM; S570, Hitachi, Inc., Mountain View, CA) at an accelerating voltage of 20 kV and a working distance of 15 mm).

EWC of poly(Dex-MA-*co*-AEMA) scaffolds was calculated according to Eq. (1). Samples were allowed to swell for 1 week in order to reach equilibrium and were then dehydrated by freeze-drying.

$$\mathrm{EWC} = \frac{w_h - w_d}{w_h} \times 100\%, \quad (1)$$

where w_h is the hydrated mass and w_d the dry mass of the poly(Dex-MA-*co*-AEMA) scaffolds.

2.6. Amine content in poly(Dex-MA-co-AEMA)

In order to confirm the copolymerization of Dex-MA and AEMA, the amine concentration was characterized first qualitatively and then quantitatively for select samples. The ninhydrin assay was used to qualitatively compare the copolymerization of 10 wt% Dex-MA and 0.1, 0.25 or 0.5 wt% AEMA either in the absence or presence of 5 wt% PEG. A solution of 0.2% (w/v) ninhydrin in ethanol was sprayed on poly(Dex-MA-*co*-AEMA) scaffolds and hydrogels and the samples were left at room temperature for ~2 h. Poly(Dex-MA-*co*-AEMA) hydrogels and scaffolds were compared for purple coloration. Poly(Dex-MA) hydrogels and scaffolds were used as controls. Based on these qualitative results, quantitative analysis was performed on only 0.5 wt% AEMA hydrogels and scaffolds because the deepest coloration was observed here. Freeze-dried samples of poly(Dex-MA-*co*-AEMA) synthesized with 10 wt% Dex-MA and 0.5 wt% AEMA (in the presence or absence of 5 wt% PEG) were analyzed by elemental analysis (Guelph Chemical Laboratories Ltd, Guelph, Ont.)

2.7. Cell and neurite penetration of scaffolds

DRGs were isolated from embryonic day 9–11 (E9–11) chicks as previously described [60] and cultured in Eagle's minimum essential medium (MEM) containing 10% horse serum, 1% glutamine, 1% penicillin/streptomycin and 50 ng/ml NGF (all supplied by Invitrogen Corp.).

Poly(Dex-MA-*co*-AEMA) scaffolds were cut into discs with a thickness of approximately 3 mm, disinfected in 70% ethanol for 20 min, and rinsed in MEM. The discs were immersed overnight in a solution of 50 μg/ml laminin (Invitrogen Corp.) and 0.01% poly-L-lysine (Invitrogen Corp.). The samples were then washed with 10% horse serum in MEM and stored at 4 °C overnight. DRG cells were plated onto the discs with a cell density of 1×10^5 cells/cm^2 and incubated at 37 °C for 3 d. The cells in the scaffolds were fixed with formaldehyde and stained with Alexa Fluor 488 phalloidin (Molecular Probes, Burlington, Ont.). Samples were embedded in 5 wt% agarose and cut into 300-μm sections using a Vibratome® Series 1000 (Technical Products International Inc., St. Louis, MO). Each section was observed under a Ziess Axiovert 100 inverted microscope (Carl Zeiss Canada Ltd., Toronto, Ont.). Images were captured using a digital camera and analyzed using SPOT software (Diagnostic Instruments, Eagan, MN) to map the 3-D cell penetration.

2.8. Peptide modification of poly(Dex-MA-co-AEMA) hydrogels

Hydrogels composed of 10 wt% Dex-MA/0.5 wt% AEMA were prepared in the absence of PEG by casting between two parallel plates. Transparent poly(Dex-MA-*co*-AEMA) disks of 5 mm in diameter and 1 mm in thickness were used for chemical modification with one of two different peptide combinations: (1) HOOC–C**RGDS**–NH_2 or (2) HOOC–CDPG**YIGSR**–NH_2/HOOC–CQAAS**IKVAV**–NH_2 (1:1 w/w) using sulfo-SMCC (Pierce Chemical Co, Rockford, IL). Twelve discs were placed in 1 ml of sulfo-SMCC solution (1 mg/ml, 10 mM PBS buffer pH 7.5) for 1 h, under gentle agitation. The samples were washed 3 times with PBS then immersed in the peptide solution (1.5 mg/ml per peptide, 10 mM PBS buffer pH 7.5) and gently agitated overnight. The samples were then washed 3 times (3 × 1 h) with PBS under gentle agitation to remove any unreacted reagents.

2.9. Characterization of peptide-modified poly(Dex-MA-co-AEMA) hydrogels

The concentration of peptides covalently coupled to the hydrogels was determined by amino acid analysis by first dissolving the amino acids bound to the hydrogels and then analyzing them quantitatively using a Waters Pico-TAG Work Station (Waters Corp., Milford, MA) and a Waters Alliance 2690 Separation Module. Approximately 10 mg of freeze-dried C**RGDS**-modified and CDPG**YIGSR**/CQAAS**IKVAV**-modified samples were hydrolyzed using a 450 μl solution of 6 N HCl with 1% phenol and 50 μl of 25 μmol/ml norleucine (as internal standard). The mixture was kept at 110 °C for 24 h and then dried at 70 °C for 4–5 days. Dissolved amino acids were derivatized using phenylisothiocyanate (PITC) and then analyzed following standard amino acid analysis protocols [61,62].

The amino acid concentrations in each peptide were averaged and the average amino acid concentration was taken to be the corresponding peptide concentration. For CDPG**YIGSR**/CQAAS**IKVAV**, the peptide concentration was determined by averaging the concentration of amino acids which were unique for each oligopeptide.

2.10. Cell and neurite interaction with peptide-modified hydrogels

Prior to cell culture, all samples were disinfected in 70% ethanol for 5 min, rinsed 3 times in MEM and then stored overnight in MEM with 10% horse serum at 4 °C. Poly(Dex-MA), poly(Dex-MA-*co*-AEMA), poly(Dex-MA-*co*-AEMA)-C**RGDS** and poly(Dex-MA-*co*-AEMA)-CDPG**YIGSR**/CQAAS**IKVAV** were placed in non-treated wells of a 96 well tissue culture plate (one sample per well) and DRGs were plated at a density of 1×10^4 cells/cm^2. The plates were then incubated at 37 °C for 2 days. Positive controls comprised tissue culture well surfaces of 96-well plates coated with a 50 μg/ml laminin for 30 min. The solution was removed and the wells were air-dried prior to plating cells. Cells were visualized with an inverted microscope and analyzed after 2 days for cell adhesion by quantifying the number of adherent cells/field (averaged over 30 random fields) and neurite outgrowth by quantifying the number neurites/field (averaged over 30 random fields) using SPOT software.

To test for specificity of peptide–integrin interaction, a competitive assay was performed by pre-incubating the cells with 0.5 mg/ml of soluble peptide solution of either CDPG**YIGSR**/CQAAS**IKVAV** (1:1 w/w ratio) or C**RGDS** in serum free media (SFM) for 30 min prior plating the cells on the respective peptide-modified hydrogels.

2.11. Statistics

The statistics were performed with commercially available software program SigmaStat 3.11 (Systat Software Inc., Richmond, CA). All experimental results are reported as mean ± standard error. For multiple comparisons, one-way ANOVA was performed using Bonferroni *t*-test. Student's *t*-test was used to make pair-wise comparisons. In all tests a *p*-value of <0.05 was regarded as significant.

3. Results

Poly(Dex-MA-*co*-AEMA) macroporous scaffolds and hydrogels were synthesized in the presence and absence of PEG, respectively, to investigate cell penetration and cell-interaction. Poly(Dex-MA-*co*-AEMA) hydrogels were modified with cell-adhesive peptides using the amine functional group of AEMA and characterized for neuronal cell adhesion and neurite outgrowth.

3.1. Morphology of poly(Dex-MA-co-AEMA) scaffolds

Fig. 1 shows the morphology of the macroporous poly(Dex-MA-*co*-AEMA) scaffolds obtained when polymerized in the presence of PEG where the liquid–liquid immiscibility of PEG and dextran lead to the macroporous geometry, as was previously observed with other dextran scaffolds [36]. As shown in Fig. 1, the macroporous geometry of poly(Dex-MA) scaffolds (Fig. 1(A)), is

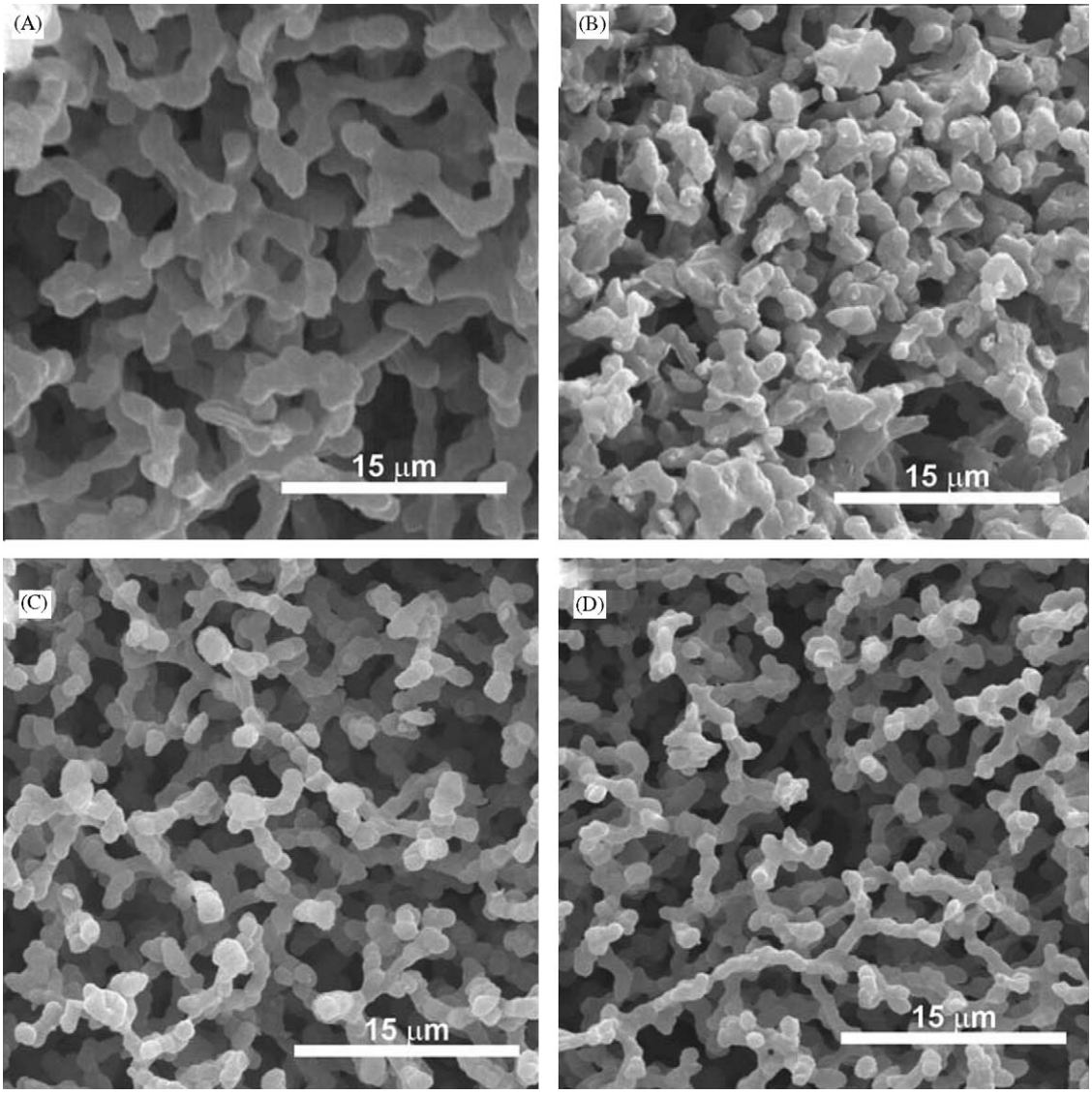

Fig. 1. Representative scanning electron micrographs of dextran hydrogels obtained by the copolymerization of 10 wt% Dex-MA 6 kDa DS 10 with AEMA in presence of 5 wt% PEG 10 kDa solutions: (A) 0 wt% AEMA, (B) 0.1 wt% AEMA, (C) 0.25 wt% AEMA, and (D) 0.5 wt% AEMA.

replicated in Figs. 1(B–D) of poly(Dex-MA-*co*-AEMA) synthesized with 0.1, 0.25, and 0.5 wt% AEMA, respectively. Although the "beaded" wall morphology of the poly(Dex-MA-*co*-AEMA) appears smaller than that of poly(Dex-MA), the introduction of the aminated monomer into the polymerization did not affect the overall macroporous structure.

3.2. Equilibrium water content of poly(Dex-MA-co-AEMA) scaffolds

The EWC of all hydrogels and scaffolds was greater than 91%, as summarized in Table 1. The EWC of poly(Dex-MA-*co*-AEMA) hydrogels were significantly different from poly(Dex-MA) ($p<0.001$); only 0.25% and 0.5% AEMA content hydrogels were significantly different from each other ($p<0.001$). Similarly, the EWC of poly(Dex-MA-*co*-AEMA) scaffolds was significantly different from that of poly(Dex-MA) ($p<0.001$); however the EWC of poly(Dex-MA-*co*-AEMA) scaffolds were not significantly different from each other.

Table 1
Equilibrium water content (EWC) of dextran hydrogels obtained by the copolymerization of 10 wt% Dex-MA 6 kDa DS 10 with AEMA in the absence or presence of 5 wt% PEG 10 kDa solutions

AEMA (wt%)	EWC (%)	
	0 wt% PEG (hydrogels)	5 wt% PEG (scaffolds)
0	92.9±0.1	94.0±0.1
0.1	92.0±0.1	91.7±0.3
0.25	92.2±0.1	91.8±0.1
0.5	91.7±0.2	91.4±0.5

3.3. Qualitative and quantitative analysis of the amine content

Qualitative analysis of the amine content was performed using a ninhydrin test to show that AEMA was successfully copolymerized with Dex-MA. The presence of amines in the gels was confirmed by the development of a purple coloration caused by the reaction of ninhydrin with the α-amino groups of AEMA (see Fig. 2). Hydrogels and scaffolds obtained with 10 wt% Dex-MA and 0, 0.01, 0.025 or 0.5 wt% AEMA showed an increasing concentration of purple intensity, with the brightest purple being observed with poly(Dex-MA-*co*-AEMA) having 0.5 wt% AEMA, which was then used in further studies. The amine concentration in these poly(Dex-MA-*co*-AEMA) hydrogels and scaffolds, quantified by elemental analysis, was found to be $36.1 \pm 0.4\,\mu mol/cm^3$.

3.4. DRG cell and neurite penetration into poly(Dex-MA-co-AEMA) scaffolds

The penetration of DRG neurons into poly(Dex-MA-*co*-AEMA) scaffolds was investigated after 3 days. Cell somas were found inside the scaffolds to a depth of up to 600 μm, demonstrating their applicability to tissue engineering. As is often observed with complex, macroporous scaffolds, their opacity made images difficult to capture.

3.5. Peptide modification of poly(Dex-MA-co-AEMA) hydrogels

CRGD**S** and CDPG**YIGSR**/CQAAS**IKVAV** peptides were immobilized to poly(Dex-MA-*co*-AEMA) hydrogels and quantified by amino acid analysis. The peptide density was calculated to be $2.6 \pm 0.9\,\mu mol/cm^3$ for **C**RGD**S**, $2.2 \pm 0.3\,\mu mol/cm^3$ for CDPG**YIGSR**, $1.9 \pm 0.2\,\mu mol/cm^3$ for CQAAS**IKVAV** ($n = 3$). The concentrations of immobilized peptides are not significantly different ($p = 0.681$).

3.6. Cell and neurite interaction with peptide-modified hydrogels

Cell adhesion and neurite outgrowth of primary DRG neurons were compared after 2 days of culture on poly (Dex-MA-*co*-AEMA)-C**RGD**S, poly(Dex-MA-*co*-AEMA)-CDPG**YIGSR**/CQAAS**IKVAV** relative to poly(Dex-MA-*co*-AEMA) and poly(Dex-MA) hydrogel controls. As shown in Fig. 3, the average number of cells/ field (averaged over 30 random fields) increased with AEMA incorporation over poly(Dex-MA) ($p < 0.001$) and further with peptide modification over poly(Dex-MA-*co*-AEMA) and poly(Dex-MA) ($p < 0.001$). Interestingly, there was no significant difference in number of adherent cells on surfaces modified with C**RGD**S vs. those modified with CDPG**YIGSR**/CQAAS**IKVAV**. The difference in cell adhesion to the hydrogel surfaces modified with peptides vs. poly(Dex-MA-*co*-AEMA) and poly(Dex-MA) is shown in Fig. 4. As shown in Fig. 5, the average number of neurites/field (averaged over 30 random fields) was greater

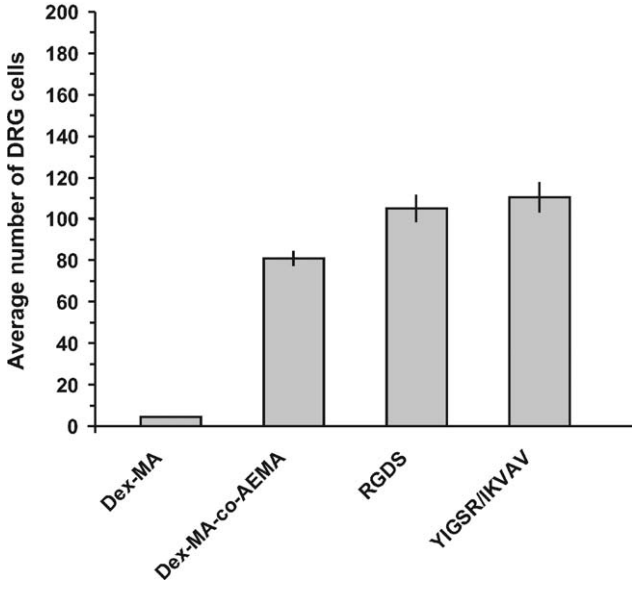

Fig. 3. Average number of DRG cells adhered on modified dextran/field (one field = 1 mm^2) for 30 random fields per hydrogel on day 2 after plating, seeding density = 2×10^4 cells/cm^2.

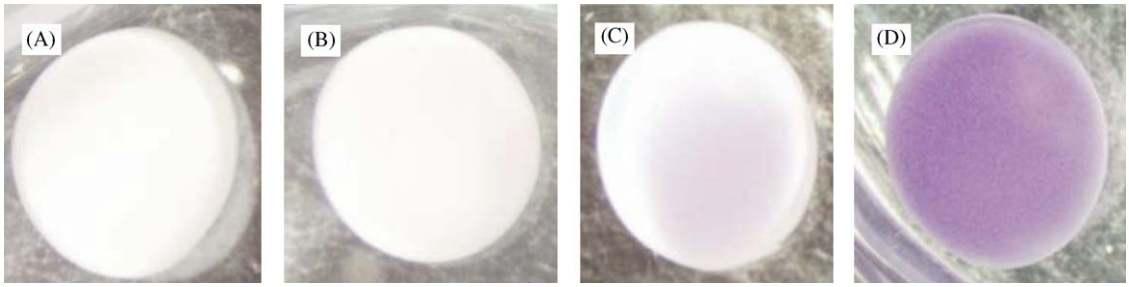

Fig. 2. Dextran hydrogels (10 wt% Dex-MA 6 kDA) synthesized with increasing concentrations of AEMA were stained with ninhydrin. An increase in the intensity of the purple ninhydrin color qualitatively demonstrated an increase in amine concentration: (A) 0 wt% AEMA, (B) 0.1 wt% AEMA, (C) 0.25 wt% AEMA, and (D) 0.5 wt% AEMA.

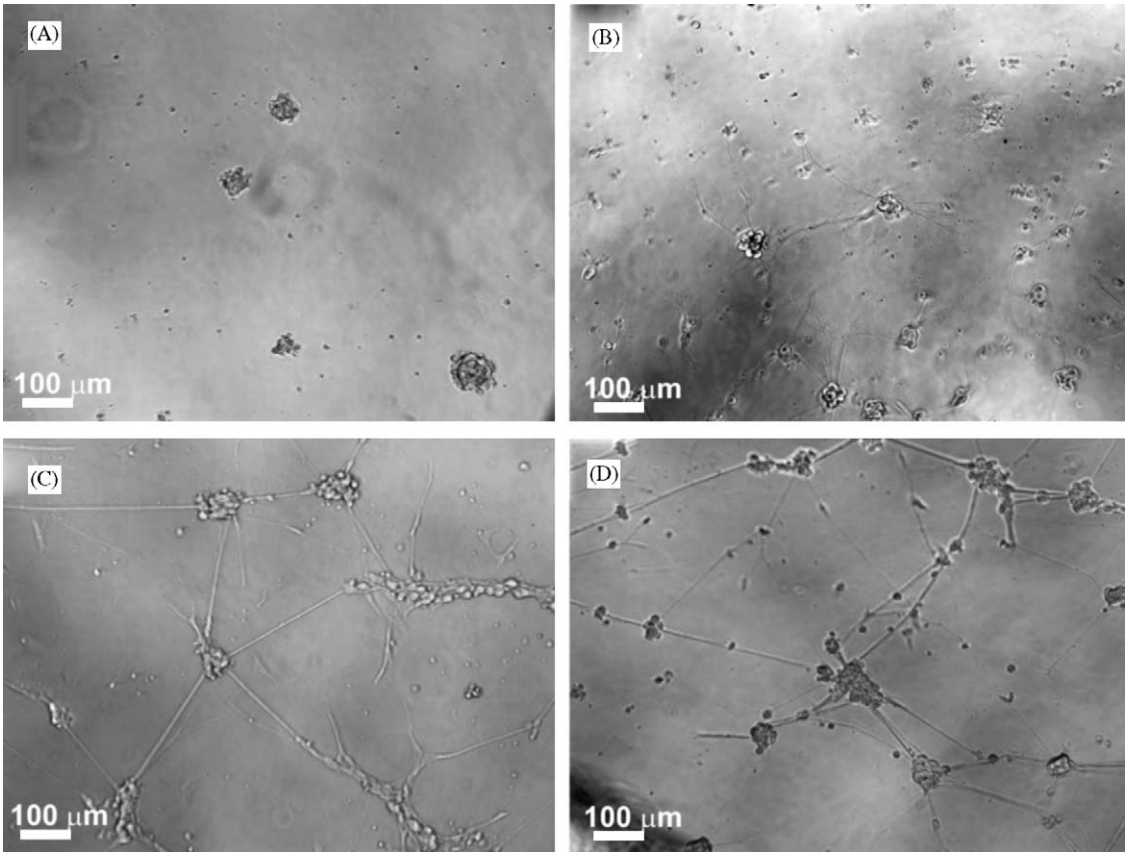

Fig. 4. Representative images captured under a light microscope of DRG neurons (plated at 2×10^4 cells/cm^2) on dextran hydrogel surfaces demonstrate adhesion and neurite extension after 2 days in culture: (a) poly(Dex-MA); (b) poly(Dex-MA-*co*-AEMA); (c) poly(Dex-MA-*co*-AEMA) modified with CG**RGD**S; and (d) poly(Dex-MA-*co*-AEMA) modified with CDPG**YIGSR**/CQAAS**IKVAV**.

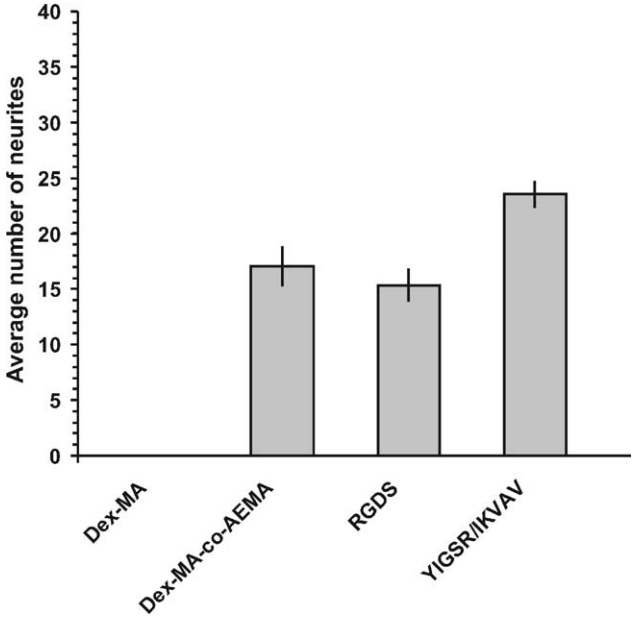

Fig. 5. Average number of neurites/field (one field = 1 mm^2) for 30 random fields per hydrogel on day 2 after plating (only neurites longer than the cell body were counted), seeding density = 2×10^4 cells/cm^2.

on poly(Dex-MA-*co*-AEMA) and peptide-modified hydrogels than on poly(Dex-MA) hydrogels, with a significant difference noted between CDPG**YIGSR**/CQAAS**IKVAV**-modified surfaces and the others studied.

To test the specificity of the interaction between cells and peptide-modified hydrogels, cells were pre-incubated with soluble cell-adhesive peptides prior to plating. Fig. 6 shows the cell adhesion (Fig. 6(A)) and neurite outgrowth (Fig. 6(B)) when pre-incubating the cells with soluble cell-adhesion peptides before plating. Significantly fewer cells adhered to the peptide-modified hydrogel surfaces when pre-incubated with soluble peptides prior to plating relative to those cells simply plated on peptide-modified hydrogels ($p < 0.001$). Similarly, significantly fewer neurites were observed on cells pre-incubated with soluble peptides prior to plating than those cells simply plated on peptide-modified hydrogels ($p < 0.001$).

4. Discussion

Several scaffolds have been synthesized with cell-adhesive peptides and shown to promote cell-specific interactions; however, only one group has successfully demonstrated peptide modification with dextran [34,35]

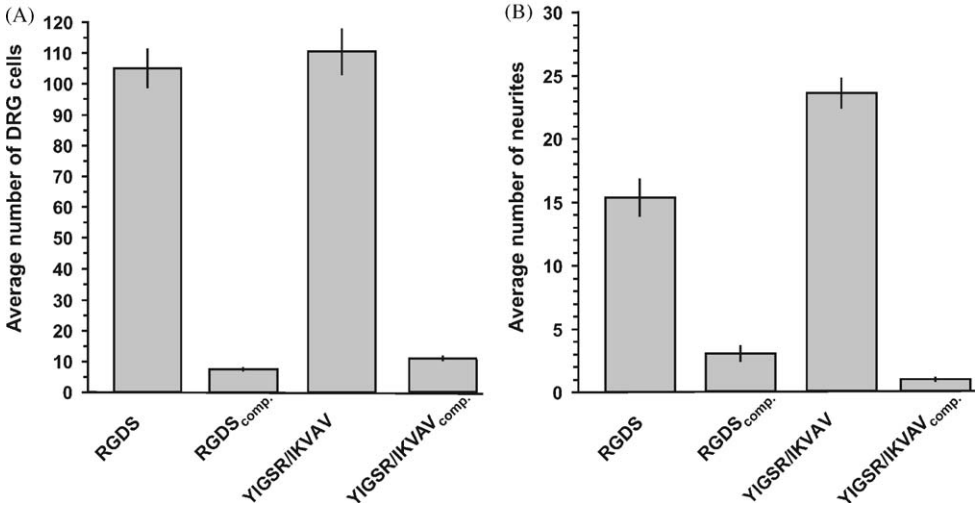

Fig. 6. (A) Average number of DRG cells adhered on modified dextran/field and (B) average number of neurites/field for 30 random fields per hydrogel on day 2 after plating and in competitive assays (comp) after pre-incubating the cells with soluble peptides. (Only neurites longer than the cell body were counted; one field = 1 mm^2, seeding density = 2×10^4 cells/cm^2, comp = DRGs pre-incubated with soluble peptides.)

and the chemistry therein, i.e., reacting primary amines of peptides with hemiacetals of oxidized dextran, would not maintain the amino acid sequence activity of our peptides of interest (i.e. IKVAV) due to side reactions with pendant primary amines of lysine (K). This would limit cellular interaction by decreased ligand-receptor recognition. Thus, in order to take advantage of the fundamental hydrogel scaffold properties of dextran, it was necessary to develop chemistry to allow defined peptide modification while preserving scaffold structure.

To this end, Dex-MA was copolymerized with a small amount of AEMA. The AEMA provides reactive primary amine groups that allow site-specific peptide immobilization using sulfo-SMCC coupling chemistry and cysteine-terminated peptides. A similar approach was previously used to covalently bind peptides to poly(hydroxyethyl methacrylate) hydrogel scaffolds, thereby enhancing cell adhesion [49]. The previously reported method for the synthesis of macroporous poly(Dex-MA) hydrogels was used to obtain poly(Dex-MA-*co*-AEMA) scaffolds and hydrogels [36]. While the poly(Dex-MA-*co*-AEMA) scaffolds synthesized with up to 0.5 wt% AEMA, had a similar macroporous morphology as poly(Dex-MA) scaffolds, the smaller beads observed by SEM in the poly(Dex-MA-*co*-AEMA) scaffolds may account for the small, yet statistically significant, difference in water content. Notwithstanding the small differences in morphology and water content, cells penetrated the poly(Dex-MA-*co*-AEMA) scaffold within the first 600 μm (after 3 days). Thus copolymerization of Dex-MA with AEMA allowed the macroporous geometry of the scaffolds to be preserved while promoting cellular interaction. The presence of AEMA in the scaffolds was further confirmed by ninhydrin, elemental analysis and peptide modification.

For tissue engineering, a combination of physical and chemical cues is important to stimulate cell adhesion and neurite outgrowth [63]. The poly(Dex-MA-*co*-AEMA) macroporous scaffold provides the physical scaffold for cell penetration and the coupled peptides promote specific cellular interactions. Cell adhesion is often the first step in a cascade of events influencing the cell fate leading to differentiation, migration, proliferation or apoptosis. Peptide modification has been used to influence cell adhesion and can be achieved by adsorption to the surface [64], incorporation into the bulk during processing [65] and/or covalent immobilization [44,45,49,52,55]. The latter provides the most stable system and was pursued here using cysteine-terminated peptides coupled via sulfo-SMCC to AEMA primary amines in the dextran hydrogel. This chemoselective technique ensures that the peptide sequence and the conformation/orientation are preserved in order to maintain integrin receptor recognition.

When poly(Dex-MA), poly(Dex-MA-*co*-AEMA), CDPG**YIGSR**/CQAAS**IKVAV**-modified, and C**RGDS**-modified hydrogels were tested for cell adhesion and neurite outgrowth, introduction of primary amines through AEMA improved cell adhesion (vs. Dex-MA), which is consistent with previous reports on the non-specific interaction between amine functionalized materials and cells [66,67] and more specifically neurons [68]. The amine groups, which are positively charged at physiological pH, interact with the negatively charged glycocalyx present on the cell surfaces. Peptide modification further enhanced cell adhesion relative to poly(Dex-MA-*co*-AEMA); however, the improvement was not as great as we had anticipated. Similar results were observed with cells cultured on aminopropyltriethoxysilane self-assembled monolayers (SAMs) and RGD-modified aminopropyltriethoxysilane SAMs [66,69,70] where no significant difference in adhesion was observed, yet the cellular activity following adhesion was significantly different on the peptide-modified surfaces. We also observed a significant difference in cellular activity, as measured by neurite outgrowth, on peptide-modified hydrogels vs.

amine-functionalized controls. The greatest neurite outgrowth was observed on CDPG**YIGSR**/CQAAS**IKVAV**-modified hydrogels. While the CDPG**YIGSR**/CQAAS**IKVAV**-modified hydrogel had twice as much total peptide as that modified with CG**RGDS**, given the similar results obtained for cell adhesion, the major driver for the greater neurite outgrowth observed is likely associated with the specificity of the interaction for cell adhesion of YIGSR and neurite outgrowth of IKVAV. This is consistent with previous findings where RGD and YIGSR were found to promote cellular adhesion and IKVAV to promote neurite outgrowth [35,43,58]. Moreover, cell integrin recognition of the peptide-modified hydrogel was confirmed with the competitive assay, thereby confirming the importance of the specificity of the interaction.

5. Conclusions

A new dextran hydrogel scaffold was synthesized by copolymerizing Dex-MA and AEMA resulting in a macroporous, cell-adhesive and cell-penetrable scaffold. Covalent modification with ECM-derived peptides enhanced cell adhesion and neurite outgrowth due to specific cell-material interactions. The greatest neurite outgrowth was observed on poly(Dex-MA-*co*-AEMA) hydrogels modified with CPDG**YIGSR** and CQAAS**IKVAV**. In ongoing studies we are investigating these materials in neural tissue-engineering applications.

Acknowledgments

We are grateful to Ms. Irene Ying and Dr. Ying Fang Chen for performing some of the cell culture experiments and to Mr. Rey Interior for the amino acid analysis (Advanced Protein Technology Centre, The Hospital for Sick Children, Toronto). We thank the Natural Sciences and Engineering Research Council of Canada (MSS), the Advanced Regenerative Tissue Engineering Center (an ORDCF-funded center), Matregen Corp and the Fonds québécois de la recherche sur la nature et les technologies (SGL) for financial support.

References

[1] Porath J, Flodin P. Gel filtration: a method for desalting and group separation. Nature 1959;183:1657–9.
[2] Bollag DM. Gel-filtration chromatography. Methods Mol Biol 1994;36:1–9.
[3] Bollag DM. Ion-exchange chromatography. Methods Mol Biol 1994;36:11–22.
[4] Shibusawa Y. Surface affinity chromatography of human peripheral blood cells. J Chromatogr B Biomed Sci Appl 1999;722:71–88.
[5] Cunningham JM, Hodgson HJ. Microcarrier culture of hepatocytes in whole plasma for use in liver support bioreactors. Int J Artif Organs 1992;15:162–7.
[6] Pawlowski R, Szigeti V, Loyd R, Przybylski RJ. Primary culture of chick embryo skeletal muscle on dextran microcarrier. Eur J Cell Biol 1984;35:296–303.
[7] Hirtenstein M, Clark J, Lindgren G, Vretblad P. Microcarriers for animal cell culture: a brief review of theory and practice. Dev Biol Stand 1980;46:109–16.
[8] Ferreira L, Gil MH, Cabrita AM, Dordick JS. Biocatalytic synthesis of highly ordered degradable dextran-based hydrogels. Biomaterials 2005;26:4707–16.
[9] Bos GW, Hennink WE, Brouwer LA, den Otter W, Veldhuis TF, van Nostrum CF, et al. Tissue reactions of in situ formed dextran hydrogels crosslinked by stereocomplex formation after subcutaneous implantation in rats. Biomaterials 2005;26:3901–9.
[10] Zhang XZ, Wu DQ, Chu CC. Synthesis and characterization of partially biodegradable, temperature and pH sensitive Dex-MA/PNIPAAm hydrogels. Biomaterials 2004;25:4719–30.
[11] Ferreira L, Rafael A, Lamghari M, Barbosa MA, Gil MH, Cabrita AM, et al. Biocompatibility of chemoenzymatically derived dextran-acrylate hydrogels. J Biomed Mater Res A 2004;68:584–96.
[12] Ferreira L, Gil MH, Dordick JS. Enzymatic synthesis of dextran-containing hydrogel. Biomaterials 2002;23:3957–67.
[13] Chiu H, Lin Y, Hsu Y. Effects of acrylic acid on preparation and swelling properties of pH-sensitive dextran hydrogels. Biomaterials 2002;23:1103–12.
[14] De Groot CJ, Van Luyn MJA, Van Dijk-Wholthuis WNE, Cadee JA, Plantinga JA, Den Otter WD, et al. In vitro biocompatibility of degradable dextran-based hydrogels tested with human fibroblasts. Biomaterials 2001;22:1197–203.
[15] Kim SH, Chu CC. Pore structure analysis of swollen dextran-methacrylate hydrogels by SEM and mercury intrusion porosimetry. J Biomed Mater Res 2000;53:258–66.
[16] Cadee JA, van Luyn MJA, Brouwer LA, Plantinga JA, van Wachem PB, de Groot CJ, et al. In vivo biocompatibility of dextran-based hydrogels. J Biomed Mater Res 2000;50:397–404.
[17] Draye JP, Delaye B, Van de Voorde A, Van Den Bulcke A, De Reu B, Schacht E. In vitro and in vivo biocompatibility of dextran dialdehyde cross-linked gelatin hydrogel films. Biomaterials 1998;19:1677–87.
[18] Trudel J, Massia SP. Assessment of the cytotoxicity of photocrosslinked dextran and hyaluronan-based hydrogels to vascular smooth muscle cells. Biomaterials 2002;23:3299–307.
[19] Kosmala J, Henthorn D, Brannon-Peppas L. Preparation of interpenetrating networks of gelatin and dextran as degradable biomaterials. Biomaterials 2000;21:2019–23.
[20] Kim SH, Won CY, Chu CC. Synthesis and characterization of dextran–maleic acid based hydrogel. J Biomed Mater Res 1999;46:160–70.
[21] Hennink WE, Cadee JA, de Jong SJ, Franssen O, Stenekes RJH, Talsma H, et al. Molecular design of biodegradable dextran hydrogels for controlled release of proteins. In: Chiellini E, Sunamoto J, Migliaresi C, Ottenbrite R, Cohn D, editors. Biomedical polymers and polymer therapeutics. New York: Kluwer Academic/Plenum Publishers; 2001. p. 3–18.
[22] Hennink WE, De Jong SJ, Bos GW, Veldhuis TFJ, van Nostrum CF. Biodegradable dextran hydrogels crosslinked by stereocomplex formation for the controlled release of pharmaceutical proteins. Int J Pharm 2004;277:99–104.
[23] Kim SH, Chu CC. In vitro release behavior of dextran–methacrylate hydrogels using doxorubicin and other model compounds. J Biomater Appl 2000;15:23–46.
[24] Saxena BB, Singh M, Gospin RM, Chu CC, Ledger WJ. Efficacy of nonhormonal vaginal contraceptives from a hydrogel delivery system. Contraception 2004;70:213–9.
[25] Stenekes RJH, Loebis AE, Fernandes CM, Crommelin DJA, Hennink WE. Controlled release of liposomes from biodegradable dextran microspheres: a novel delivery concept. Pharm Res 2000;17:690–5.
[26] Stenekes RJ, Loebis AE, Fernandes CM, Crommelin DJ, Hennink WE. Degradable dextran microspheres for the controlled release of liposomes. Int J Pharm 2001;214:17–20.

[27] Brondsted H, Andersen C, Hovgaard L. Crosslinked dextran—a new capsule material for colon targeting of drugs. J Control Release 1998;53:7–13.
[28] Hovgaard L, Brondsted H. Dextran hydrogels for colon-specific drug delivery. J Control Release 1995;26:159–66.
[29] Cortesi R, Esposito E, Osti M, Squarzoni G, Menegatti E, Davis SS, et al. Dextran cross-linked gelatin microsphere as a drug delivery. Eur J Pharm Biopharm 1999;47:153–60.
[30] Mehvar R. Dextrans for targeted and sustained delivery of therapeutic and imaging agents. J Control Release 2000;69:1–25.
[31] Zhang Y, Chu CC. Biodegradable dextran–polylactide hydrogel networks: their swelling, morphology and the controlled release of indomethacin. J Biomed Mater Res 2002;59:318–28.
[32] Osterberg E, Bergstrom K, Holmberg K, Riggs JA, Vanalstine JM, Schuman TP, et al. Comparison of polysaccharide and poly(ethylene glycol) coatings for reduction of protein adsorption on polystyrene surfaces. Colloids Surf A Physicochem Eng Aspects 1993;77:159–69.
[33] Massia SP, Stark J, Letbetter DS. Surface-immobilized dextran limits cell adhesion and spreading. Biomaterials 2000;21:2253–61.
[34] Massia SP, Stark J. Immobilized RGD peptides on surfaces-grafted dextran promote biospecific cell attachment. J Biomed Mater Res 2001;56:390–9.
[35] Massia SP, Holecko MM, Ehteshami GR. In vitro assessment of bioactive coatings for neural implant applications. J Biomed Mater Res 2004;68A:177–86.
[36] Levesque SG, Lim RM, Shoichet MS. Macroporous interconnected dextran scaffolds of controlled porosity for tissue-engineering applications. Biomaterials 2005;26:7436–46.
[37] Hubbell JA. Materials as morphogenetic guides in tissue engineering. Curr Opin Biotechnol 2003;14:551–8.
[38] Hirano Y, Mooney DJ. Peptide and protein presenting materials for tissue engineering. Adv Mater 2004;16:17–25.
[39] Lutolf MP, Hubbell JA. Synthetic biomaterials as instructive extracellular microenvironments for morphogenesis in tissue engineering. Nat Biotechnol 2005;23:47–55.
[40] Shin H, Jo S, Mikos AG. Biomimetic materials for tissue engineering. Biomaterials 2003;24:4353–64.
[41] Zhang N, Yan H, Wen X. Tissue-engineering approaches for axonal guidance. Brain Res Rev 2005;49:48–64.
[42] Adams DN, Kao EYC, Hypoliye CL, Distefano MD. Growth cone turn and migrate up an immobilized gradient of laminin IKVAV peptide. J Neurobiol 2005;62:134–47.
[43] Schense J, Bloch J, Aebisher P, Hubbell JA. Enzymatic incorporation of bioactive peptides into fibrin matrices enhances neurite extension. Nat Biotechnol 2000;18:415–9.
[44] Suzuki M, Itoh S, Yamaguchi I, Takakuda K, Kobayashi H, Shinomiya K, et al. Tendon chitosan tubes covalently coupled with synthesized laminin peptides facilitate nerve regeneration in vivo. J Neurosci Res 2003;72:646–59.
[45] Dhoot NO, Tobias CA, Fischer I, Wheathley MA. Peptide-modified alginate surfaces as a growth permissive substrate for neurite outgrowth. J Biomed Mater Res 2004;71A:191–200.
[46] Shaw D, Shoichet MS. Toward spinal cord injury repair strategies: peptide surface modification of expanded poly(tetrafluoroethylene) fibers for guided neurite outgrowth in vitro. J Craniofac Surg 2003;14:308–16.
[47] Tong YW, Shoichet MS. Enhancing the neuronal interaction on fluoropolymer surfaces with mixed peptides or spacer group linkers. Biomaterials 2001;22:1029–34.
[48] Luo Y, Shoichet MS. A photolabile hydrogel for guided three-dimensional cell growth and migration. Nat Mater 2004;3:249–53.
[49] Yu TT, Shoichet MS. Guided cell adhesion and outgrowth in peptide-modified channels for neural tissue engineering. Biomaterials 2005;26:1507–14.
[50] Zhang Z, Yoo R, Wells M, Beebe TP, Biran R, Tresco P. Neurite outgrowth on well-characterized surfaces: preparation and characterization of chemically and spatially controlled fibronectin and RGD substrates with good bioactivity. Biomaterials 2005;26:47–61.
[51] Schense J, Hubbell JA. Three-dimensional migration of neurites is mediated by adhesion site density and affinity. J Biol Chem 2000;275:6813–8.
[52] Rowley JA, Madlambayan G, Mooney DJ. Alginate hydrogels as synthetic extracellular matrix materials. Biomaterials 1999;20:45–53.
[53] Fittkau MH, Bezuidenhout D, Lutolf MP, Human P, Hubbell JA, Davies N. The selective modultation of endothelial cell mobility on RGD peptide containing surfaces by YIGSR peptides. Biomaterials 2005;26:167–74.
[54] Shu XZ, Gosh K, Liu Y, Palumbo FS, Luo Y, Clark RA, et al. Attachment and spreading of fibroblasts on an RGD peptide-modified injectable hyaluronan hydrogel. J Biomed Mater Res 2003;68A:365–75.
[55] Ho MH, Wang DM, Hsieh HJ, Liu HC, Hsien TY, Lai JY, et al. Preparation and characterization of RGD-immobilized chitosan scaffolds. Biomaterials 2005;26:3197–206.
[56] Kam L, Shain W, Turner JN, Bizios R. Selective adhesion of astrocytes to surfaces modified with immobilized peptides. Biomaterials 2002;23:511–5.
[57] Gunn JW, Turner SD, Mann BK. Adhesive and mechanical properties of hydrogels influence neurite extension. J Biomed Mater Res 2005;72A:91–7.
[58] Saneinejad S, Shoichet MS. Patterned poly(chlorotrifluoroethylene) guides primary nerve cell adhesion and neurite outgrowth. J Biomed Mater Res 2000;50:465–74.
[59] van Dijk-Wolthuis WNE, Tsang SKY, Kettenes-van den Bosch JJ, Hennink WE. A new class of polymerizable dextrans with hydrolyzable groups: hydroxyethyl methacrylated dextran with and without oligolactate spacer. Polymer 1997;38:6235–42.
[60] Nishi R. Autonomic and sensory neuron cultures. Methods Cell Biol 1996;51:49–63.
[61] Cohen SA, Strydom DJ. Amino acid analysis utilizing phenylisothiocyanate derivatives. Anal Biochem 1988;174:1–16.
[62] Heinrikson RL, Meredith SC. Amino acid analysis by reverse-phase high-performance liquid chromatography: precolumn derivatization with phenylisothiocyanate. Anal Biochem 1984;136:65–74.
[63] Schmidt CE, Leach JB. Neural tissue engineering: strategies for repair and regeneration. Annu Rev Biomed Eng 2003;5:293–347.
[64] Satriano C, Manso M, Gambino GL, Rossi F, Marletta G. Adsorption of a cell-adhesive oligopeptide on polymer surfaces irradiated by ion beams. Biomed Mater Eng 2005;15:87–99.
[65] Ernsting MJ, Bonin GC, Yang M, Labow RS, Santerre JP. Generation of cell adhesive substrates using peptide fluoralkyl surface modifiers. Biomaterials 2005;26:6536–46.
[66] Lee MH, Brass DA, Morris RJ, Composto RJ, Ducheyne P. The effect of non-specific interactions on cellular adhesion using model surfaces. Biomaterials 2005;26:1721–30.
[67] Faucheux N, Schweiss R, Lutzow K, Werner C, Groth T. Self-assembled monolayers with different terminating groups as model substrates for cell adhesion studies. Biomaterials 2004;25:2721–30.
[68] Stenger DA, Pike CJ, Hickman JJ, Cotman CW. Surface determinants of neuronal survival and growth on self-assembled monolayers in culture. Brain Res 1993;630:136–47.
[69] Cavalcant-Adam EA, Shapiro IM, Composto RJ, Macarak EJ, Adams CS. RGD peptides immobilized on a mechanically deformable surface promote osteoblast differentiation. J Bone Miner Res 2002;17:2130–40.
[70] El-Ghannam AR, Ducheyne P, Risbud M, Adams CS, Shapiro IM, Castner D, et al. Model surfaces engineered with nanoscale roughness and RGD tripeptides promote osteoblast activity. J Biomed Mater Res A 2004;68:615–27.